Identification of various chemical phenomena in concrete using thermal analysis

R Vedalakshmi[a], A Sundara Raj[b] & N Palaniswamy[a]

[a]Corrosion Protection Division, [b]Characterization and Measurement Division,

Central Electrochemical Research Institute, Karaikudi 630 006, India

Email: corrveda@yahoo.co.in

Chemical changes that occur in concrete at the microstructure level due to environmental effects are normally identified by SEM, XRD, thermal analysis and by chemical analysis. In the present investigation, the chemical compounds formed in various chemical reactions are quantified using thermal analysis. The concrete having characteristic compressive strength of 20 MPa was subjected to undergo various chemical reactions for a specified period. Three types of cements were used for casting the concrete specimens. The thermal analyses (DTA and TG) were carried out on powdered concrete samples passing through 75 μm sieve drawn from the concrete specimens which were subjected to various chemical phenomenon. Chemical compounds such as $Ca(OH)_2$, gypsum, ettringite, calcium chloroaluminate are estimated quantitatively. The type of fly ash blended with cement and complex amine salt in Migrating Corrosion Inhibitor (MCI) treated concrete are also identified. Each chemical compound is identified by a distinct endotherm present in the DTA (Differential Thermal Analysis) plot and quantitative estimation has been done using the TG (Thermo-gravimetric) curve.

Keywords: Chemical changes, Thermal analysis, Pozzolanic reaction, Sulphate attack, Friedel's salt, Migrating corrosion inhibitor

Concrete is a widely used construction material and it undergoes chemical changes with time when exposed to various environments. It attains strength only after completion of sufficient hydration reaction of cement with water. Similarly it deteriorates due to ingress of various aggressive species such as sulphates, chlorides and carbon-di-oxide. Each of these species reacts with either hydrated cement compounds (Calcium hydroxide, C-S-H) or with cement compounds (C3A) and forms insoluble compounds[1-4]. All these chemical changes occur at the microstructure level and are identified by Scanning electron microscope (SEM) with EDAX, X-ray diffractometry (XRD) and thermal analysis[1,5-9]. SEM, X-ray imaging and other optical methods need expensive surface preparation; by XRD method quantities of material less than 2 or 3% of the total can be rarely identified[10-12].

Thermal analysis is widely used in studies on concrete to determine the hydration reaction of cement/blended cement accurately by estimating calcium hydrates and $Ca(OH)_2$ content[13-15]. The application is extended to identify the various deterioration phenomena of concrete[1,5,6]. The respective weight-losses can be obtained from the corresponding TG curve, which in turn allows the quantification of different phases. It is important to note that the high resolution of the thermal analysis experiment allows quantification of even very minor components and does not need any expensive surface preparation.

In the present study, using thermal analysis, various chemical compounds formed during (i) pozzolanic reaction of blended cements, (ii) hydrated cement products reacted with chlorides and sulphates (iii) CaO content of fly ash blended with PPC (iv) presence of migrating corrosion inhibitor in concrete were estimated.

Experimental Procedure

Materials

20 MPa concrete was used throughout the investigation. The mix proportions used for casting the concrete specimens are given in Table 1. Three types of cement such as Ordinary Portland cement (OPC) conforming to I.S.8119, Portland pozzolana cement (PPC) conforming to I.S. 2340, Portland slag cement (PSC) conforming to I.S. 450 were used. In pozzolana and slag cements, Portland cement was replaced with 25% fly ash and 50% slag respectively. Chemical composition of cements used is given as

Table 1 — Details of mix proportion

Type of cement	W/C ratio	Cement (kg/m^3)	Water (kg/m^3)	Fine aggregate (kg/m^3)	Coarse aggregate (kg/m^3)	28 day compressive strength (MPa)	Slump (mm)
OPC	0.67	284	190	770	1026	27	50
PPC	0.67	284	190	770	1026	23	60
PSC	0.67	284	190	770	1026	28	10

Table 2 — Chemical composition of three cements

Compound	Types of cement		
	Ordinary Portland cement, (%)	Portland Pozzolana cement, (%)	Portland slag cement, (%)
Silicon -di-oxide(SiO_2)	20-21	28-32	26-30
Aluminium oxide (Al_2O_3)	5.2-5.6	7.0-10.0	9.0-11.0
Ferric oxide (Fe_2O_3)	4.4-4.8	4.9-6.0	2.5-3.0
Calcium oxide (CaO)	62.-63	41-43	44-46
Magnesium oxide (MgO)	0.5-0.7	1.0-2.0	3.5-4.0
Sulphur - tri-oxide (SO_3)	2.4-2.8	2.4-2.8	2.4-2.8
Loss on ignition	1.5-2.5	3.0-3.5	1.5-2.5

Table 3 — Grading of coarse and fine aggregate

Coarse aggregate		Fine aggregate	
Sieve size (mm)	Cumulative % retained	Sieve size (mm)	Cumulative % retained
20	0	4.75	0
16	25	2.36	12
12.5	52	0.600	49
10	72	0.300	85
4.75	100	0.150	97
		<0.150	100

Table 2. Well-graded river sand and good quality crushed blue granite were used as fine and coarse aggregates respectively. The different size fractions of coarse aggregate (20 mm down graded and 12.5 mm down graded) were taken and recombined to a specified grading as shown in Table 3. In mix proportion, cement content and water/cement (w/c) ratio were kept constant for both blended cement concrete and Portland cement concrete. Potable water was used for casting the concrete. Cubical concrete specimens of size 100 mm^3 were cast.

Pozzolanic reaction of blended cements

To determine the pozzolanic reaction of blended cements, cubical concrete specimens of the three cements were kept immersed in potable water for 28, 90 and 365 days. At the end of each curing period, the cubes were broken and samples were collected for thermal analysis. After performing the DTA analysis, the Ca(OH)$_2$ content and additional calcium hydrates content formed during the pozzolanic reaction were quantitatively estimated.

The reduction of permeability due to the formation of additional hydrates in PPC and PSC concretes is ensured by determining the co-efficient of water absorption and chloride penetration. Co-efficient of water absorption was determined as per procedure given in ASTM C642 by oven drying method[16]. The experiment was conducted using 100 mm size cubical concrete specimens at three curing periods namely 7, 28 and 90 days.

For determining the chloride penetration, the concrete specimens of size 450x250x150 mm (LxBxD) were cast using three cements. After 28 days of curing, 3% NaCl solution was ponded on the top of the each specimens for 4 days and allowed to dry for 3 days. This alternate wetting and drying cycle was continued for 30 months and after that the specimen was broken and sliced to different depths from the top to bottom. The samples collected from the different depths were powdered and sieved through 150 μm sieve and the water soluble chloride was determined by Mohr's method[17].

Estimation of calcium oxide content of fly ash in blended cement

According to the chemical composition of fly ash, the type of fly ash is divided into low calcium fly ash and high calcium fly ash. In low calcium fly ash, the CaO content is less than 10% whereas in high calcium fly ash, it is more than 10%. In factory produced Portland pozzolana cement, the type of fly ash blended is not known. This can be identified using thermal analysis by estimating Ca(OH)$_2$ content. Three pozzolana cements from three different factories (sample B, C, D) were used. Cubical concrete specimens (100 mm size) were cast using each cement sample and cured in potable water for 28

days. At the end of 28 days, the compressive strength was determined. After this, the samples were collected from the concrete cubes for thermal analysis.

Effect of sulphate attack

The hydrated cement products react with sulphate and form two major expansive products such as gypsum and ettringite. For quantifying these products, 100 mm size cubical concrete specimens were cast using three cements and cured for 28 days. After curing, the specimens were kept immersed in 10% $MgSO_4$ solution. At the end of 9 and 15 months, the samples were collected from the top surface of the cube i.e up to 3 mm, and thermal analysis was carried out. The extent of deterioration was also determined periodically by measuring the decrease in compressive strength.

Friedel's salt formation

When concrete is exposed to chloride environment, the C_3A phase in the concrete reacts with chloride and forms Friedel's salt. In concrete this may be in the form of either bound chloride or water-soluble free chloride. For determining the bound chloride, 1% chloride was added at the time of casting. After 28 days of curing, the specimens were exposed in the exposure yard and salt solution was sprayed periodically. After exposure of 24 months, the cubes were broken and samples were collected from the center of the specimen. The results were compared with the concrete in which neither chloride was added nor exposed to salty environment.

Presence of migrating corrosion inhibitor (MCI)

Two alkanolamine based MCIs such as diethanolamine and triethanolamine were taken and migration of inhibitors was studied using diffusion test cell. Using 20 MPa concrete, the concrete disk of size 85 mm dia and 25 mm thick were cast and cured for 28 days. After curing, the concrete disk was fixed between the anodic and cathodic compartment of diffusion test cell as shown in Fig. 1. The anodic compartment contains saturated calcium hydroxide + 200 mM concentration of diethanolamine/triethanol-amine whereas cathodic compartment contains saturated calcium hydroxide+3% NaCl solution. With time the inhibitor migrate from the anodic compartment to the cathodic compartment through the concrete disk. In cathodic compartment the efficiency of the migrated inhibitor in presence of chloride was

evaluated by conducting the Tafel extrapolation technique periodically at the end of 1, 5, 20 and 25 days. Steel specimen having an area of 1 cm^2 was polished and kept immersed in the cathodic compartment through the hole as shown in Fig. 1. Using saturated calomel electrode as a reference electrode and platinum as an auxiliary electrode, the specimen was polarized from −200 to +200 mV from the corrosion potential. Using Solarron Model No.1295 the potentiodynamic polarization was carried out at a scan rate of 1 mV/s. E versus log I plot was drawn and from that, the corrosion current as well as corrosion rate were calculated. At the end of the experiment, the concrete disk was powdered and thermal analysis was carried out.

Since the amount of inhibitor present in the concrete disk is normally very low, to identify the clear distinct endotherm in the DTA plot, the above two inhibitors were added at the concentration of 3% by weight of cement at the time of concrete casting. Using 20 MPa concrete, 100 mm size cubical concrete specimens were cast and kept immersed in potable water for 28 days. At the end of 28 days the cubes were broken and samples were collected for thermal analysis.

Sample preparation for thermal analysis

Samples were powdered in silica mortar and sieved through 75 μm sieve. About 1 g of sample was collected in a closed plastic container. TG/DTA were done using Polymer laboratories (UK), Thermal Science Division STA 1500 thermal analyser. It has a microbalance with a resolution of 0.01 mg. Type R thermocouple (Pt-13% Rh/Pt) is used for temperature measurements in this instrument. The sample was taken in a ceramic crucible and heated from the room temperature to 800°C at a heating rate of 20°C/min using air as a medium under static condition. Alumina powder was used as the reference material. Both TG/DTA were done simultaneously. The upper temperature was mainly limited because of
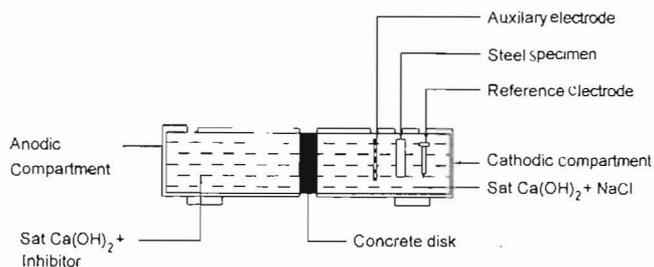
Fig. 1 — Schematic diagram of diffusion test cell.

crystallization of hydrated compounds at higher temperature. In the case of sulphate deteriorated concrete sample and inhibitor added sample the upper temperature was limited to 600°C. The data are presented in the form of TG/DTA plot. The chemical compound which undergoes dehydration reaction at a particular temperature has been identified by a distinct endotherm in the DTA plot. Using TG curve, the quantity of compound has been estimated.

Results and Discussion

Quantification of pozzolanic reaction of blended cements

Typical plots of TG/DTA curves for the sample collected at the end of 90 days in 20 MPa concrete are given in Figs 2 and 3. From the DTA curves, it can be seen that each curve consists of three zones. Zone one between 100-300°C which is attributed to the dehydration of C-S-H and ettringite[18]. The temperature at which the dehydration of these compounds vary depending upon the available CaO: SiO$_2$ in the hydrated cement matrix. The peak observed around 350°C denotes the formation of Fe$_2$O$_3$ solution[19]. Zone two (290-350°C) characterizes the decomposition of calcium aluminate silicate hydrate, calcium aluminate hydrate and calcium chloroaluminate[20]. The third zone (450-510°C) is attributed to the dehydration of calcium hydroxide. Intensity of endothermic peak in OPC is more when compared to PPC and PSC. An endotherm around 700°C indicates the decarbonation of calcium carbonate in the hydrated compound.

Estimation of Ca(OH)$_2$ content

The sharp endotherm in the DTA curve around 465°C indicates the decomposition of Ca(OH)$_2$ formed during hydration[21]. The Ca(OH)$_2$ was estimated from the weight-loss measured from the TG curve between the initial and final temperature of the corresponding peak by considering the following decomposition reaction[6]:

$$Ca(OH)_2 \longrightarrow CaO + H_2O \qquad \qquad ...(1)$$

Estimation of calcium hydrates content

The total weight-loss including that due to loss of water from other hydrates was measured from the difference in weight between 100 and 600°C[22]. The calcium hydrates content which is a total of calcium silicate hydrate, calcium aluminate hydrate and calcium sulfoaluminate hydrate formed during hydration was calculated by deducting calcium hydroxide content from total weight-loss[23].

Table 4 compares the Ca(OH)$_2$ content and calcium hydrates content in 20 MPa concrete at the end of 28, 90 and 365 days. From the table, it can be seen that in PPC and PSC concrete, Ca(OH)$_2$ content decreases with time whereas in OPC concrete it increases with
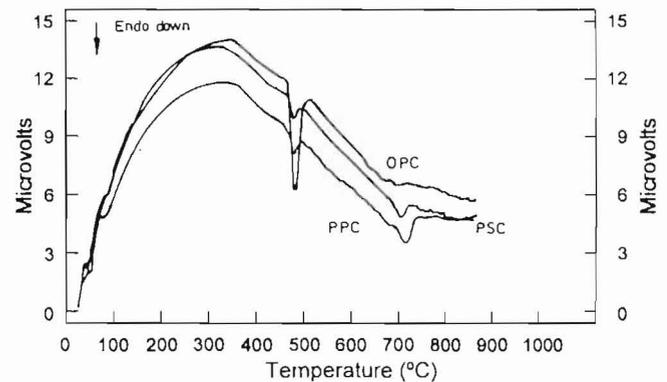
Fig. 2 — DTA curves of three cements in 20 MPa concrete after 90 days of curing
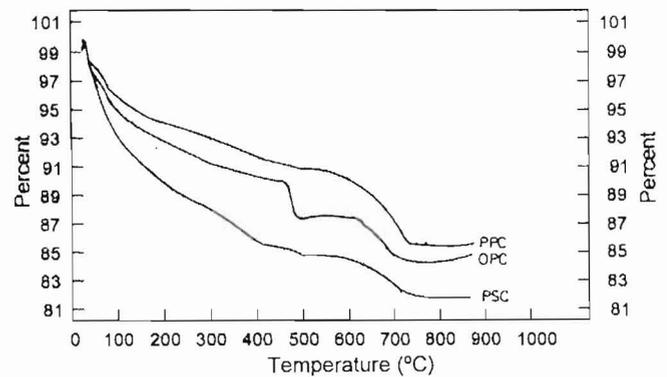
Fig. 3 — TG curves of three cements in 20 MPa concrete after 90 days of curing

Table 4 — Estimation of Ca(OH)$_2$ content and calcium hydrates content

Type of cement	At the end of 28 days		At the end of 90 days		At the end of 365 days	
	Ca(OH)$_2$ content (%)	Calcium hydrates (%)	Ca(OH)$_2$ content (%)	Calcium hydrates (%)	Ca(OH)$_2$ content (%)	Calcium hydrates (%)
OPC	6.17	5.19	9.17	5.36	12.05	6.04
PPC	5.34	5.46	2.14	5.22	1.38	7.53
PSC	2.06	7.56	2.59	8.07	0.304	8.33

time. The reduction in $Ca(OH)_2$ content in blended cement concrete indicates its consumption during pozzolanic reaction. The data emphasis that in PPC and PSC concretes, lime is consumed whereas in OPC concrete, lime is produced.

It is also observed that the calcium hydrates content is more in PPC and PSC concrete than OPC concrete and it increases with time up to 365 days. For example in PPC concrete it is 5.46% at the end of 28 days and increased to 7.53% at the end of 365 days. Similarly in PSC concrete, the value is 7.56% and 8.38% at the end of 28 and 365 days respectively. This clearly shows that in blended cement concrete, in the presence of water both fly ash and slag react with $Ca(OH)_2$ and form secondary calcium hydrates (both aluminate hydrate and silicate hydrate). The reactions are called as 'pozzolanic reaction' and given below:

$$3Ca(OH)_2 + Fly\ ash + H_2O \longrightarrow 3CaO.2SiO_2.3H_2O ...(2)$$
$$(Secondary\ C\text{-}S\text{-}H)$$

$$3Ca(OH)_2 + Slag + H_2O \longrightarrow 3CaO.2SiO_2.3H_2O + 4CaO.Al_2O_3.3H_2O ...(3)$$
$$(C\text{-}S\text{-}H) \qquad (C\text{-}A\text{-}H)$$
$$(Secondary\ C\text{-}S\text{-}H\ and\ C\text{-}A\text{-}H)$$
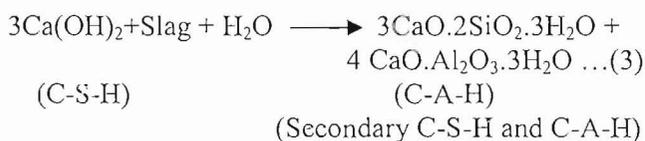
These additional secondary hydration products are not formed in OPC concrete as indicated by the lower value. When compared to PPC concrete, PSC concrete has more hydrates because of higher alumina and calcium oxide content of slag in Portland slag cement.

Water and chloride penetration

From Table 5 it can be seen that in all the three curing periods, the co-efficient of water absorption in blended cement concrete is less than in OPC concrete. Similarly from the Table 6, it can be seen that when compared to OPC concrete, the chloride content is less in all depths in PPC and PSC concrete. The above results confirm that the additional secondary calcium hydrates densify the pore structure in PPC and PSC concretes and cause the reduction of permeation of chloride and water.

Identification of type of fly ash blended with Portland Pozzolana cement

In Portland pozzolana cement, the $Ca(OH)_2$ content depends upon the CaO content of the fly ash blended. Figures 4 and 5 compare the DTA and TG plot of three pozzolana cements (B,C,D) at the end of 28 days of curing respectively. From the DTA curve (Fig. 4), it can be seen that the intensity of peak is more in sample C than in sample B and D. From the TG curve (Fig. 5), the % of $Ca(OH)_2$ content is 1.07, 2.14 and 0.82% for sample B, C and D respectively. The values indicate that when compared to sample B and D, the sample C contains 2 to 2.6 times more $Ca(OH)_2$ content, which implies that either the fly ash
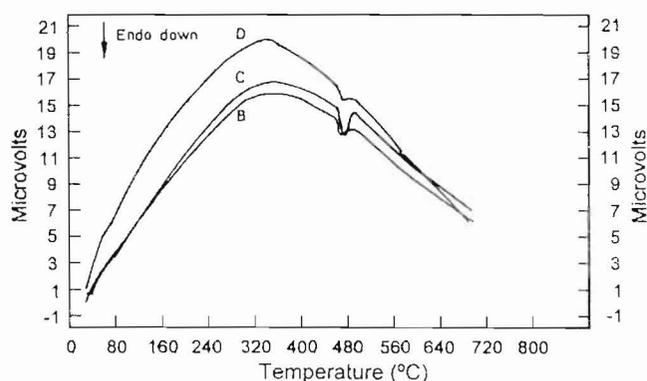
Fig. 4 — DTA curves of three pozzolana cement samples (B, C, D) of 20 MPa concrete after 28 days of curing
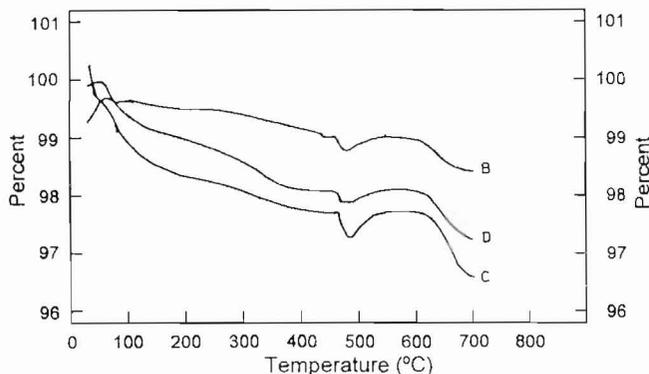
Fig. 5 — TG curves of three pozzolana cement samples (B, C, D) of 20 MPa concrete after 28 days of curing

Table 5 — Comparison of co-efficient of water absorption of 20 MPa concrete

Type of cement	Co-efficient of water absorption, $(\times 10^{-10})$ (m^2/s)		
	7 days	28 days	90 days
OPC	16.6	15.10	7.64
PPC	9.86	7.71	4.94
PSC	8.27	5.80	3.32

Table 6 — Comparison of water soluble chloride at different depths

Type of cement	Water soluble chloride (ppm)		
	30-60 mm depth	60-90 mm depth	90-120 mm depth
OPC	8307	7455	7029
PPC	5751	5751	4899
PSC	4686	4899	5538

blended is high calcium fly ash or its calcium content is marginally more than the other two cement samples. This is confirmed by determining compressive strength at the end of 28 days. For sample C it is 45.2 MPa whereas for sample B and D it is 38.3 and 39.2 MPa respectively. In OPC concrete it is 47.37 MPa. It has been reported[24,25] that the strength development of high calcium fly ash added concrete is comparable to that of OPC concrete whereas in low calcium fly ash added concrete, the strength development is lower than that of OPC concrete.

Quantification of gypsum and ettringite formation

When concrete is exposed to sulphate bearing environment, the permeation of sulphate ions causes the formation of sulphate bearing phases such as ettringite and gypsum in the internal microstructure. This causes cracking and subsequently leads to significant reduction in strength[26-28]. The reactions are as follows:

$$MgSO_4 + Ca(OH)_2 + 2H_2O \longrightarrow CaSO_4.2H_2O+ Mg(OH)_2 \quad ...(4)$$

$$MgSO_4 + CaO.SiO_2.3H_2O + H_2O \longrightarrow CaSO_4.2H_2O+ Mg(OH)_2+ SiO_2.H_2O ...(5)$$

$$Mg(OH)_2+SiO_2.H_2O \longrightarrow MgO.SiO_2.H_2O + H_2O...(6)$$
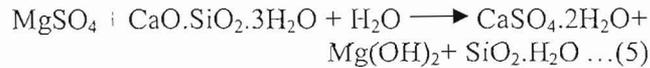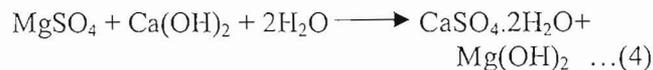
When compared to sodium sulphate attack, magnesium sulphate attack is more severe on concrete. From Eqs (4)-(6), it can be seen that magnesium ions directly react with C-S-H and thus reduces the binding property of the concrete matrix. It has been reported that gypsum exists in crystalline form and ettringite in amorphous form[1,29] in concrete. These expansive products are quantified by XRD, SEM with EDAX and thermal analysis[9,30]. Wee *et al.*[30] reported that since the ettringite is in amorphous form and could not be detected through XRD but detected by thermal analysis. The dehydration of ettringite and gypsum formation was indicated by endothermic peaks at 80-100°C and 110-130°C respectively[5,9,30,31].

Figures 6 and 7 compare the DTA curves of three cements in 20 MPa concrete after 9 and 15 months of exposure in 10% MgSO4 solution. From Fig. 6 (after 9 months of exposure) it can be seen that, OPC concrete shows only ettringite peak whereas PPC and PSC concretes show both ettringite and gypsum peaks. In OPC concrete, because of higher C₃A

content all the gypsum formed is converted into ettringite and this is evident from the large intensity of the peak. In the case of blended cements because of reduction of C₃A content (dilution effect) the intensity of the ettringite peak is weak when compared to OPC concrete but gypsum peak is strong.

As shown in Fig. 7, in all the three cements, only gypsum peak is observed after 15 months of exposure. The intensity of the peak is more than that after 9 months of exposure. This indicates that with exposure secondary ettringite is not formed and gypsum formation is the only expansive product.

Using TG curve, the gypsum and ettringite were estimated quantitatively and the results are given in Table 7. From the data it can be inferred that the gypsum formation increases with exposure period irrespective of type of cement. It is more in PSC concrete than in PPC and OPC concretes. This is also confirmed by observing the reduction in compressive strength in PSC concrete (Table 8) whereas increase in compressive strength in other two concretes at the end of 15 months of exposure. Table 8 compares the change in compressive strength of three cements up to
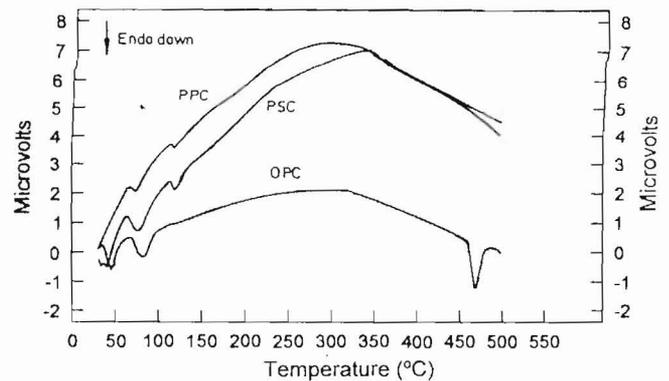
Fig. 6 — DTA curves of three cements in 20 MPa concrete after 9 months of exposure in 10% MgSO₄ solution.
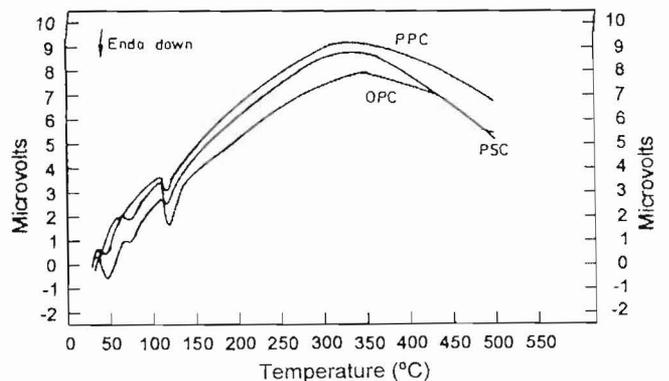
Fig. 7 — DTA curves of three cements in 20 MPa concrete after 15 months of exposure in 10% MgSO₄ solution.

Table 7 — Estimation of gypsum and ettringite

Type of cement	After 9 months of exposure				After 15 months of exposure		
	Gypsum	Ettringite	Compressive strength, MPa		Gypsum	Compressive strength, MPa	
			Water	10% MgSO$_4$		water	10% MgSO$_4$
OPC	–	3.90	36	39	5.33	37	43
PPC	1.19	1.79	33	38	3.53	38	41
PSC	3.87	4.42	30	33	7.21	33	31

36 months. From this it can be seen that both PPC and PSC concrete show more reduction in compressive strength than OPC concrete at the end of 36 months. The magnesium ions attack directly C-S-H gel because of reduction of Ca(OH)$_2$ in blended cements and thus get deteriorated more.

Estimation of bound chlorides (Friedel's salt) present in the chloride contaminated concrete

In chloride-induced corrosion, the dissolvable chloride concentration that actually resides in the pore solution and is permanently in contact with the steel surface determines the initiation and rate of corrosion of rebar. The tricalcium aluminate phase (C$_3$A) of cement has the ability to complex the dissolvable chloride resulting in the formation of calcium chloro-aluminate hydrate (3 CaO.Al$_2$O$_3$.CaCl$_2$.10H$_2$O) and possibly ferrite analogue (3CaO.Fe$_2$O$_3$.CaCl$_2$.10H$_2$O), according to the following reaction:

$$3CaO.Al_2O_3 + 2NaCl + Ca(OH)_2 + 10H_2O \longrightarrow$$

$$3CaO.Al_2O_3.CaCl_2.10\ H_2O + 2NaOH \ ...(7)$$
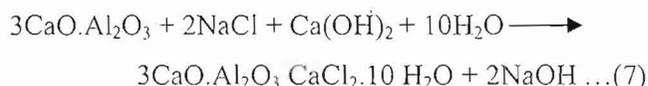
The formation of this bound chlorides results in the reduction of corrosion inducing dissolvable chlorides in the pore solution and hence lowering the corrosion risk. The amount of C$_3$A content present in the cement influences the amount of bound chlorides in concrete[32,33].

It is observed in thermal analysis that around 370^{0}C, the chloride is disassociated into water and calciumchloro aluminate as per the following reaction[34].

$$3CaO.Al_2O_3.CaCl_2.10H_2O \longrightarrow$$

$$3CaO.Al_2O_3.CaCl_2 + 10H_2O \ ...(8)$$
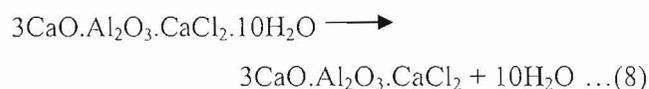
Figure 8 compares the DTA curves of 20 MPa concrete containing no chloride with 1% added chloride. In 1% chloride added concrete, an endothermic peak at 375°C is observed whereas no

Table 8 — Variation of compressive strength with exposure period in 10% MgSO$_4$ solution

Type of cement	Exposure period (months)					
	6	9	15	21	30	36
OPC	38	39	43	34	37	39
PPC	37	38	41	43	36	30
PSC	34	33	31	33	27	16
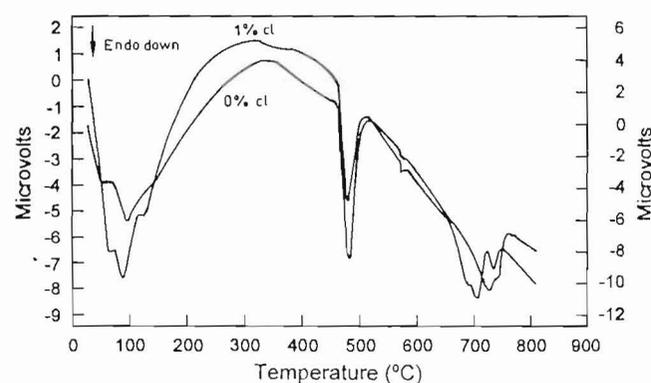
Fig. 8 — Comparison of DTA curves of 1% and 0% chloride contaminated concrete

endothermic peak at this temperature in 0% chloride added concrete. From the TG curves, it is estimated that the weight-loss as per equation 8 is 1.14% by weight of the sample.

Identification of presence of migrating corrosion inhibitors in concrete

Migrating corrosion inhibitor (MCI) technology was developed to protect the steel rebar in concrete. Alkanolamine with carboxylate compounds are used as migrating corrosion inhibitors. These can be incorporated as an admixture or can be used by surface impregnation of existing concrete structures. With surface impregnation, diffusion transports the MCIs into deeper concrete layer, where they inhibit the onset of rebar corrosion[35-38]. The presence of these inhibitors in concrete is quantified by ion- exchange
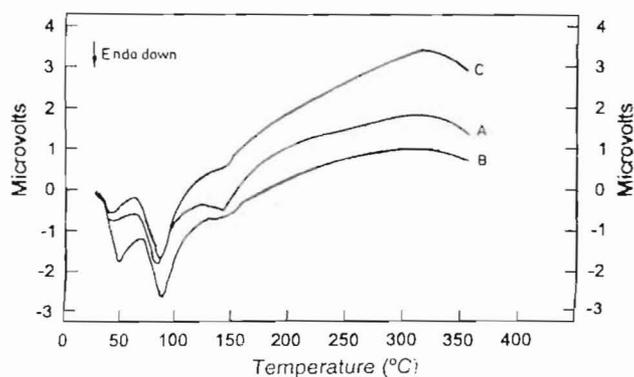
Fig. 9 — Comparison of DTA curves diethanolamine (DE) and triethanolamine (TE) added/diffused in concrete A. Diethanolamine (added) B. Trithenolamine (added) C. Amine (diffused)

Table 9 — Comparison of corrosion rate of steel in diffusion test using Tafel extrapolation technique

Duration (Days)	Sat. Ca(OH)$_2$ + 200 mM DEA		Sat. Ca(OH)$_2$ + 200 mM TEA	
	I_0 (A/m^2)	Corrosion rate (mmpy)	I_0 (A/m^2)	Corrosion rate (mmpy)
1	1.088	1.2621	0.7622	0.8908
5	0.4597	0.5332	0.6145	0.7129
20	0.2716	0.3150	0.3004	0.3485
25	0.1316	0.1527	0.1044	0.1211

chromatography[39]. Because of complex salt formation volumetric method can not be used and it has been identified using thermal analysis.

In Fig. 9, curves A and B represent the presence of diethanolamine (DEA) and triethanolamine (TEA) which were added in concrete whereas curve C represents the presence of inhibitors in concrete disk through diffusion (under diffusion test). All the three curves show an endothermic peak at 140^0C, which may be due to the complex salts formed by inhibitors with cement compounds. The amount of inhibitor present in the added form is more than the same diffused through the concrete disk and this is clearly indicated by the strong intensity of the peak in curve A and B than in curve C.

From Table 9, it can be seen that the initial corrosion rate of 1.2621 mmpy of steel specimen gets reduced with time and attains a value of 0.1527 mmpy at the end of 25 days. This indicates that the DEA in the anodic compartment diffuses through the concrete disk with time and causes the reduction of corrosion rate of steel specimen kept in the cathodic compartment. The corrosion rate at the end of 25 days

is 8.3 times less than the corrosion rate at the end of 1 day. Similarly studies conducted on TEA also show that it diffuses through the concrete disk and causes 7.3 times reduction of corrosion rate at the end of 25 days. Electrochemical data confirms the diffusion of both inhibitors through the concrete disk

Conclusions

Based on the results of the study the following conclusions can be drawn:

(i)   The chemical changes occurring in concrete due to the intrusion of chlorides, sulphates can be *quantitatively estimated by thermal analysis.*

(ii) Presence of migrating corrosion inhibitors, pozzolanic reaction of blended cements, high and low calcium fly ash can be also identified by this method.

References

1   Brown P W & Doerr A, *Cem Concr Res,* 30 (2000) 411.
2   Glass G K, Page C L & Short N R, *Corros Sci,* 32 (1991) 1283.
3   Lawrence C D, *Mag Concr Res,* 42 (1990) 249.
4   Rasheeduzzafar, *ACI Mater J,* 89 (1992) 574.
5   DongXu L I, Yimin Chen, Jiaohua Su & Xuequanug, *Cem Concr Res,* 30 (2000) 881.
6   Dweck J, Buchler P M, Coelho A C V & Cartledge F K, *Thermochim Acta,* 346 (2000) 105.
7   Dhir R K, Jhones M R & Ahmed H H, *Cem Concr Res,* 20 (1990) 579.
8   Tutti K, *Corrosion of Steel in Concrete* (Swedish Cement and Concrete Research Institute, Stockholm), 1982, 46.
9   Manu Santhanam, Cohen C D & Olek J, *Cem Concr Res,* 33 (2003) 325.
10   Stutzman P E, *Application of scanning electron micr in cement and concrete petrography* In ASTM STP-····, Petrography of Cementitious Materials, edited by S Dehayes & D Stark, 1993, 74.
11   Struble L & Stutzman P E, *J Mater Sci Lett,* 8 (1989) 632.
12   Stuzman P E & Clifton J R, *Proc 21st Int Conf on Cement Microscopy,* Las Vegas, Nevada, 1999, 10.
13   Slanika T, Madej T & Jakubekov D, *Thermochim Acta,* 93 (1985) 601.
14   Vedalakshmi R, Sundara Raj A, Srinivasan S & Ganesh Babu K, *Thermochim Acta,* 2003, 4·.
15   Bhatty J I, Dollimore D, Gamlen G A, Mangabhai R J & Olmez H, *Thermochim Acta,* 106 (1986) 115.
16   ASTM C642-80. Standard test method for specific gravity, absorption and voids in hardened concrete. ASTM standards, 1995, V.04.02, 318-319.
17   Mangat P S & Molly B T, *Cem Concr Res,* 21 (1996) 27
18   Lea F M, *The Chemistry of Cement and Concrete,* 4th edn (London Edward Arnold), 1974, 184.

19 Monzo J Paya, Borrachero J M V, Peris-Mora E & Velazquez P, *7th CANMET/ACI Int Conf on fly ash, silica fume, slag and natural pozzolans in concrete*, SP-199, Supplementary volume, ACI Detroit, 2001, 241.

20 Ubbriaco P & Calabrese D, *Thermochim Acta*, 321 (1998) 143.

21 Hubbert Wicker W & Heidemann D, *7th CANMET/ACI Int Conf on fly ash, silica fume, slag and natural pozzolans in concrete*, SP-199, Vol. 1, ACI, Detroit, 2001, 83.

22 Singh S P, *National Conference on Thermal Analysis*, Vol. 1 BARC, Mumbai, India, 2002, 69.

23 Taylor H T W, *Cement Chemistry*, 2nd edn (Thomas Telford, London), 1997, 102.

24 Yuan R L & Cook J E, *1st Int Conf on the use of fly ash, silica fume and other mineral by- products in concrete*, SP-79, ACI, Detriot, 1983, 307.

25 Lamond J F, *1st Int Conf on the use of fly ash, silica fume and other mineral by- products in concrete*, SP-79, ACI, Detriot, 1983, 47.

26 Rivera J Sanchez de Rojas M I & Frias M, *7th CANMET/ACI Int Conf on fly ash, silica fume, slag and natural pozzolans in concrete*, SP-199, Supplementary volume, ACI Detroit, 2001, 357.

27 Mangat P S & Khatib J M, *ACI Mater J*, 92 (1995) 542.

28 Merchand J, Samson E, MaltisY & Beaudoin J J, *Cem Concr Res*, 24 (2002) 317.

29 RILEM technical Committee 68-NMH. *Materials and Constructions*, 19 (1986) 137.

30 Wee T H, Suryavanshi A K & Wang S F, *ACI Mater J*, 97 (2000) 536.

31 Huachang, Pei Jane Huang & Hou S C, *Mater Chem Phy*, 58 (1999) 12.

32 Rasheeduzzafar, Hussain E H & Al-Saadoun S S, *Cem Concr Res*, 21(5) (1991)779.

33 Rasheeduzzafar, *ACI Mater J*, 89(6) (1992) 574.

34 Hubbard F H, *Cem Concr Res*, 15 (1985) 185.

35 Dhir R K, El-Mohr Mak & Dyer T D, *Cem Concr Res*, 26 (1996) 1767.

36 Morris W & Vazquez M, *Cem Concr Res*, 32 (2002) 259.

37 Batis G, Routoulas A & Rakanta E, *Cem Concr Comp*, 25 (2003) 109.

38 Biegovic D, Miksic B A & Stehly R D, *Mater Corros*, 51 (2000) 444.

39 SHRP Report No.SHRP-87C-102C. SHRP Report on Feasibility studies on the injection of synergistic corrosion inhibitors for protection of concrete bridge components. SHRP, USA, 1987, 1.